
EFFECT OF A PROCESS MINING BASED PRE-PROCESSING STEP IN PREDICTION OF THE CRITICAL HEALTH OUTCOMES

A PREPRINT

✉ **Negin Ashrafi**

Department of Industrial and Systems Engineering
University of Southern California
Los Angeles, CA 90089
ashrafin@usc.edu

✉ **Armin Abdollahi**

Department of Electrical Engineering
University of Southern California
Los Angeles, CA 90089
arminabd@usc.edu

✉ **Greg Placencia**

Department of Industrial and Manufacturing Engineering
California State Polytechnic University-Pomona
Pomona, CA 91768
gvplacencia@cpp.edu

✉ **Maryam Pishgar**

Department of Industrial and Systems Engineering
University of Southern California
Los Angeles, CA 90089
pishgar@usc.edu

ABSTRACT

Predicting critical health outcomes such as patient mortality and hospital readmission is essential for improving survivability. However, healthcare datasets have many concurrences that create complexities, leading to poor predictions. Consequently, pre-processing the data is crucial to improve its quality. In this study, we use an existing pre-processing algorithm, concatenation, to improve data quality by decreasing the complexity of datasets. Sixteen healthcare datasets were extracted from two databases - MIMIC III and University of Illinois Hospital - converted to the event logs, they were then fed into the concatenation algorithm. The pre-processed event logs were then fed to the Split Miner (SM) algorithm to produce a process model. Process model quality was evaluated before and after concatenation using the following metrics: fitness, precision, F-Measure, and complexity. The pre-processed event logs were also used as inputs to the Decay Replay Mining (DREAM) algorithm to predict critical outcomes. We compared predicted results before and after applying the concatenation algorithm using Area Under the Curve (AUC) and Confidence Intervals (CI). Results indicated that the concatenation algorithm improved the quality of the process models and predictions of the critical health outcomes.

Keywords Critical health outcomes · concatenation algorithm · deep learning · predictions · process mining

1 Introduction

A patient's health records can be understood as a sequence of observations including services performed, diagnoses, or lab measurements [1]. In the process mining field, each of these observations is called an event, and the sequences of observations are referred to as event logs. Process mining analyzes and optimizes processes. The process mining approach has been used widely in healthcare to enhance healthcare processes [2] and to predict critical health outcomes [1, 3, 4, 5].

Real-life event logs are complex and noisy. Infrequent behaviors and various concurrences generate inefficient and complex process model through process discovery algorithms. Healthcare data exacerbates these issues. For instance, various lab measurements can be taken at the same time causing concurrent relationships among these different lab measurement events. It is therefore critical to pre-process raw event logs to improve their quality, to make the process model more understandable.

A variety of pre-processing algorithms have been used to improve data quality [6, 7, 8]. The concatenation algorithm is a recent innovation that significantly improves event logs and process model quality for real-life benchmark datasets [7]. However, the concatenation algorithm has not been tested on real-life healthcare event logs.

Early prediction of patient health outcomes is critical to clinical decision making and effective allocation of medical resources [9]. For example, Coronary Artery Disease (CAD) causes approximately 610,000 deaths yearly in the United States alone and 17.8 millions deaths worldwide [10, 11]. Moreover, approximately, 6 million American adults over the age of 20 had heart failure (HF) between 2015 to 2018 [12, 13, 14]. This has resulted in the Centers for Medicare & Medicaid Services penalizing hospitals nearly 2.5 billion USD since 2012 for unplanned 30-day readmission rates [15]. Patient mortality for Paralytic Ileus (PI) can be as high as 40 in ICU settings [16]. In 2019, diabetes directly caused 1.5 million deaths. More recently, COVID-19, caused by the SARS-CoV-2, heavily impacted morbidity and mortality with major economic consequences [17]. These highlight the need for accurate predictions models to reduce patient mortality rates and readmission, so as to reduce financial consequences.

Many frameworks have been used to predict the critical health outcomes [18, 19]. Decay Replay Mining (DREAM) is a recent process mining / deep learning framework. It has significantly improved predicting healthcare outcomes for ICU patients with various diseases [3, 5] using raw and complex healthcare event logs. However, the effectiveness of pre-processing has not yet been studied using real life healthcare datasets. This work focuses on two issues: 1) Does pre-processing healthcare datasets improve data quality and enhance the process model? 2) Is the concatenation algorithm an effective pre-processor that predicts critical health outcomes such as patient mortality and readmissions?

The structure of this paper is as follows: Section 2 provides the preliminaries. Section 3 details the methodology used in this study. Section 4 presents the evaluation, covering Datasets, Setup, Results, and Discussion. Section 5 concludes the findings and directions for future research.

2 Preliminaries

The notations used in this section are adopted from [20].

2.1 Process Mining

Process mining analyzes and optimizes process sequences called event logs. Process mining uses the following steps: process discovery, conformance checking, and process enhancement. The process discovery step is the most important step in process mining. This step uses process discovery algorithms to output a process model, mostly called a Petri Net (PN).

2.2 Petri Net

A PN is a mathematical model often used to represent a process. It includes a set of places graphically represented as circles and transitions as rectangles. Transitions correspond to events. The occurrence of a process is modeled by firing transitions. Places can be marked or unmarked. Marked places indicate current process states. A place is marked by putting a dot (token) in the circle corresponding to that event. For a transition to be fired, all its input places must contain a token. If a transition fires, the all tokens are removed from its inputs. Also, each output of the transition receives a token.

2.3 Event Logs

An event $a \in A$ is an instantaneous change of a process' state where A is the finite set of all possible events. An event a can happen more than once in a provided process. An event instance E is a vector with two attributes at minimum: the name of the associated event a and the corresponding occurrence timestamp, τ . The timestamps τ of two events cannot be equal. A trace $g \in G$ is a finite and ordered sequence of event instances [20].

2.4 Decay Replay Mining

Decay Replay Mining (DREAM) [21] is a process mining / deep learning-based approach used to predict the next event in the sequence of a process. DREAM uses places from a process model and extends these places with a time decay function $F(\tau)$. The time decay function $F(\tau)$ uses timestamps τ information as a parameter when replaying event logs L on a process model and produces Timed State Samples (TSS).

2.5 Timed State Samples

A TSS will be produced by replaying event logs L on a process model [21]. A TSS, $S(\tau)$ at time τ results from concatenating time decay function values $F(\tau)$, token counts $C(\tau)$, and of a marking $M(\tau)$:

$$S(\tau) = F(\tau) \oplus C(\tau) \oplus M(\tau) \quad (1)$$

2.6 Concatenation Algorithm

The concatenation algorithm [7] is a pre-processing algorithm that removes some concurrences and self-loops based on a probability algorithm. This improves the quality of event logs and the resulting process model.

2.7 Concurrency Relation

Given any event logs L , and any two labels $\ell, \ell' \in L$, and any two events $e_i, e_j \in E$, a concurrent relation exists, denoted by $(e_i || e_j)$, given the following conditions: $|\ell \rightarrow \ell'| > 0$ and $|\ell' \rightarrow \ell| > 0$.

2.8 Self-loops

A self-loop exists in the event logs L , if $|\ell \rightarrow \ell|$ is positive for some event $e \in E$ with $\lambda(e) = \ell$ [22].

2.9 F-Measure

An F-Measure is an evaluation metric uses to measure the quality of a process model. The F-Measure is a trade-off value between fitness and precision [23]. The Fitness of a process model represents the behavior of the event logs L . Precision shows the capability of a model to produce the behaviors found only in the event logs L . In this work, the alignment-based method is used to measure both fitness and precision per [20, 24].

2.10 Complexity

Complexity is an evaluation metric that measures the quality of a process model. Complexity shows how easily a process model can be understood. Several metrics measure the complexity of a model [22], including Control-Flow Complexity (CFC) [23], size of the models [25], and structuredness [25]. CFC shows how many branches are prompted by split gateways in a process model. The size of a process model calculates the numbers of the nodes and arcs in the model. A process model is structured, if, for any split gateway in the process model a corresponding join gateway exists.

2.11 Split Miner

Split Miner (SM) is a process discovery algorithm that produce a sound PN from the event logs L . It produces a process model with less complexity and higher F-Measure value than other process discovery algorithms. The SM algorithm includes the following steps: First, generate a directly-follow graph and identify short loops. Second, discover the existing concurrency relation between events. Third, utilize filtering by introducing 2 threshold values, to control the filtering process (frequency threshold, ϵ), the other, η , to control concurrency relations. Moreover, the algorithm derives choice and concurrency relations by adding split gateways. In the end, the join gateways are discovered. The output of these steps is a BPMN, and it can be converted to a PN through using ProMs' BPMN Miner package [26]. This algorithm is publicly available as a java application [26].

3 Methodology

This section focuses on a proposed method for predicting several health outcomes with and without applying a pre-processing step on event logs L . First, feature selection is described. Next, conversion of Electronic Health Records (EHR) to event logs L is explained followed by the pre-processing step. Finally, the DREAM algorithm is introduced to predict health outcomes.

The intuition behind this methodology is that applying an appropriate pre-processing step on complex healthcare event logs L decreases complexity of a process model. Hence, it predicts critical health outcomes more accurately. Since healthcare event logs L contain many concurrences and self loops, applying a concatenation algorithm to concurrent events makes the process model simpler and generates more accurate predictions. An overview of the proposed framework is shown in Figure1.

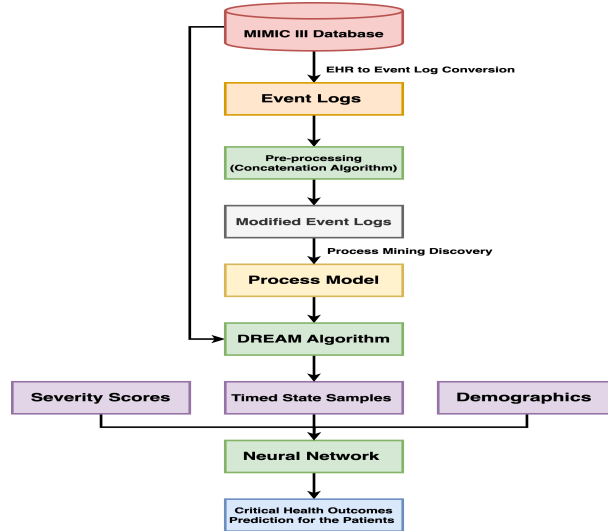


Figure 1: Overview of the Proposed Model

3.1 Feature Selection

MIMIC III [27] and University of Illinois Hospital (UIH) databases[18] were used for predictions. Due to the nature of our approach (process mining / deep learning approach) every patient must have a medical history available at the time of prediction. Table1 shows the features extracted from MIMIC III and UIH databases by disease category.

Table 1: Features Extracted from MIMIC III and UIH Databases

Data Type (Part 1)							
Type of Disease	Admission	Insurance	Lab Related	Demographics	Elixhauser Comorbidities	CPT and ICD-9-CM codes	Discharge
PI	x	x	x	x	NA	NA	x
HF	x	x	x	x	x	x	x
COVID			x	x			
Diabetes	x	x	x	x	x	x	NA
CAD	x	x	x	x	x	NA	NA

Data Type (Part 2)							
Type of Disease	Severity scores	Care unit in and out from ICU	Location	Encounter-based	Report-based	Vitals signs	ICU-based
PI	NA	x					
HF	x						
COVID			x	x	x	x	x
Diabetes	x	NA					
CAD	NA	NA					

3.2 Conversion of EHR to the Event Logs

Event logs L can be understood as a sequence of events with timestamps τ associated to events that have occurred. Events represent activities performed on patients such as admission, diagnosis, lab measurements, etc., also known as patients careflows. Each unique event has a corresponding timestamp τ when it occurred. In this paper, the timestamp τ of comorbidity and artificial events correspond to the discharge time of the corresponding hospital admission. Since events in a trace g occur sequentially, multiple comorbidities or artificial events with the same timestamps τ are delayed by multiples of 1 ms to retain their order. Table2 summarizes the conversion of the EHR to the event logs L .

Table 2: Conversion of EHR from Databases to Event Logs

MIMIC III and UIH Tables	Events
ADMISSIONS, PATIENTS	Admission type, Demographics, patient's exit type, discharge, insurance type
D_LABITEMS, LABEVENTS, ADMISSIONS	Lab events
ICUSTAYS, CALLOUT	Careunit type
LABEVENTS	Abnormal flagged events
Admissions, Diagnoses_ICD	Elixhauser Comorbidity Score events
Diagnose_ICD, Procedures_ICD, CPTevents	30 Artificial event abstractions

3.3 Pre-processing Step

In Algorithm1, the resultant event logs (L) from the previous step were then used as an input to the concatenation algorithm. Assume that events e_i, e_j, e_k , and $e_l \in L$, if $(e_i \rightarrow e_j)$ and $(e_j \rightarrow e_i)$; also $(e_k \rightarrow e_l)$ and $(e_l \rightarrow e_k)$, if there is a concurrent relations between $e_i, e_j, e_i||e_j$, and between $e_k, e_l, e_k||e_l$.

Algorithm 1 Event Log Concatenation Algorithm

Require: Event logs L , threshold p^*

Ensure: Modified event logs L'

```

1: Initialize an empty list of concurrent pairs
2: for all events  $e_i, e_j \in L$  do
3:   if  $(e_i \rightarrow e_j) \wedge (e_j \rightarrow e_i)$  then
4:     Add  $(e_i||e_j)$  to the list of concurrent pairs
5:   end if
6: end for
7: Initialize an empty list of valid pairs
8: for all pairs  $(e_i||e_j)$  in the list of concurrent pairs do
9:   if  $P(e_i \rightarrow e_j) > p^*$  and  $P(e_j \rightarrow e_i) > p^*$  then
10:     $P(e_i||e_j) = P(e_i \rightarrow e_j) + P(e_j \rightarrow e_i)$ 
11:    Add  $(e_i||e_j, P(e_i||e_j))$  to the list of valid pairs
12:   end if
13: end for
14: Sort the list of valid pairs in descending order of  $P(e_i||e_j)$ 
15: for all pairs  $(e_i||e_j)$  in the sorted list of valid pairs do
16:   Remove  $e_i$  and replace  $e_j$  with  $e_i \oplus e_j$ 
17: end for
18: for all events  $e_i \in L$  not concatenated do
19:   if  $e_i \in e_i \oplus e_j$  then
20:     Remove  $e_i$  and replace with  $e_i \oplus e_j$ 
21:   end if
22: end for
23: for all events  $e_i \in L$  do
24:   if  $e_i \rightarrow e_i$  then
25:     Remove  $e_i$ 
26:   end if
27: end for
28: Feed the modified event logs  $L'$  to the SM algorithm for process modeling
29: Use the resultant process model as input to the DREAM algorithm for prediction

```

We then calculate $P(e_i \rightarrow e_j)$ and $P(e_j \rightarrow e_i)$; and $P(e_k \rightarrow e_l)$ and $P(e_l \rightarrow e_k)$. Moreover, threshold value p^* is introduced, if $P(e_i \rightarrow e_j) > p^*$ and $P(e_j \rightarrow e_i) > p^*$, the combination is chosen. Similarly, if $P(e_k \rightarrow e_l) > p^*$ and $P(e_l \rightarrow e_k) > p^*$, the combination is chosen for the next step. Additionally, the probabilities of the selected combinations were added and sorted in the descending order, $P(e_i||e_j) = P(e_i \rightarrow e_j) + P(e_j \rightarrow e_i)$ also $P(e_k||e_l) = P(e_k \rightarrow e_l) + P(e_l \rightarrow e_k)$. Furthermore, if $P(e_i||e_j) = P(e_k||e_l)$ a re-position step was applied. After the order of combinations for concatenation is finalized, the concatenation algorithm selects the ordered combinations one by one for the concatenation. Assume that (e_i, e_j) is chosen for concatenation, event e_i is removed and replaced with the concatenated event, $e_i \oplus e_j$. This step is repeated until all selected combinations are concatenated in the event logs L .

After concatenating all combinations in the event logs L based on descending order, some events will remain that are not concatenated. Each non concatenated event will be examined and checked for event, $e_i \in e_i \oplus e_j$. In that case, e_i will be removed and replaced with $e_i \oplus e_j$. If $e_i \notin e_i \oplus e_j$, while the final trace remains unchanged. Finally, if $e_i \rightarrow e_i$ exist, it is removed. The modified event logs L was then fed to the SM algorithm to produce a process model. The resultant process model was input to the DREAM algorithm for prediction as detailed in the next subsection.

3.4 DREAM algorithm

The algorithm has three different phases [21]. The first phase is to create a PN model from an event log L and assign a decay function to each PN location $f_p(\tau)$. The discovery log is then replayed, and feature arrays comprising decay function response values, token movement counts, and resource use are extracted. Lastly, we train a Neural Network (NN) to predict the next event, using these feature arrays as training data. To simulate data values that decrease over time, one can use decay functions. Financial domains, physical systems, and population trend modeling are among the common applications for these functions. We assign a linear decay function $f_p(\tau)$ to every place in the PN produced by SM on an event log L .

Algorithm 2 PN Discovery and Decay Function Initialization

Require: Event log L with traces $\{g_1, g_2, \dots, g_n\}$

Require: Decay function parameters α, β

Ensure: Discovered PN with initialized decay functions

- 1: **Step 1: PN Model Discovery**
 - 2: Use SM to discover a PN model from event log L
 - 3: **for** each place p in the PN model **do**
 - 4: Associate place p with a linear decay function $f_p(\tau) = \max(\beta - \alpha \cdot \Delta_p, 0)$
 - 5: **end for**
 - 6: **Step 2: Decay Function Enhancement**
 - 7: **for** each place p in the PN model **do**
 - 8: Initialize the decay function $f_p(\tau)$ to 0 by setting $\Delta_p = \infty$
 - 9: **end for**
 - 10: **Step 3: Calculate Decay Rates**
 - 11: **for** each place p in the PN model **do**
 - 12: Calculate the maximum trace duration $\Delta_{\max}(L) = \max_{1 \leq i \leq |L|} (\nu_{d_{ts}}(L_{i,\gamma(L_i)}) - \nu_{d_{ts}}(L_{i,1}))$
 - 13: Define $v_p(g)$ as the number of tokens entering place p during replay of trace g
 - 14: **if** $\max_{g \in L} v_p(g) \leq 1$ **then**
 - 15: Set $\alpha_p = \frac{\beta}{\Delta_{\max}(L)}$
 - 16: **else**
 - 17: Set $\alpha_p = \frac{\beta}{\text{mean}_{g \in L} \delta_p(g)}$
 - 18: **end if**
 - 19: **end for**
 - 20: **Step 4: Update Decay Functions with Calculated Rates**
 - 21: **for** each place p in the PN model **do**
 - 22: Update the decay function $f_p(\tau) = \max(\beta - \alpha_p \cdot (\tau - \tau_p), 0)$
 - 23: **end for**
 - 24: Return the discovered PN model with initialized decay functions
-

By using $\Delta_p = \tau - \tau_p$, we can express the time difference between the current time, τ , and the most recent time a token entered place p , τ_p . With the help of the two decay function parameters, α and β , we can adjust the significance level. Based on the reactivation durations of a place p , α should ideally be set so that the slope of $f_p(\tau)$ covers the entire range from β to 0. In other words, the slope should not be excessively steep for a small Δ_p such that $f_p(\tau) = 0$ or too flat for a large Δ_p such that $f_p(\tau) = \beta$. This suggests varying α values with each place in the PN model. In the next step of Algorithm2 we try to estimate these α_p values. Using the event log L and the corresponding PN found by the SM on L , we estimate α_p . There are a limited number of event instances in each trace g in L . The j^{th} event instance of an event log L 's i^{th} trace is referred to by $L_{i,j}$. $\lambda(L_i)$ expresses the number of event instances of the i^{th} trace of the event log L . The value of the attribute d for the event instance E is $\nu_d(E)$. When an attribute d is absent from an event instance E , the result is $\nu_d(E) = 0$, an empty set. We use d_{ts} to represent the attribute timestamp. $\Delta_{\max}(L)$, the Maximum observed trace duration in an event log L , is defined in the algorithm and based on the value of $\max_{g \in L} v_p(g)$ the value of α_p is determined. If the value is less than one then α_p will be set to a value that ensures that before the final event

instance of a corresponding trace g in L occurs, the response of $f_p(\tau)$ will never equal 0. By doing this, we ensure that, until the end of a trace, we will have information about the occurrence of a particular event in the decay function's response. However, when the value of $\max_{g \in L} v_p(g)$ is larger than one we calculate the average time it takes for a place p to reactivate. With this knowledge, we adjust the decay rate so that, for the average time between reactivations, $f_p(\tau)$ yields a level of recent token movement importance.

Algorithm 3 Event Log Replay and Feature Extraction

Require: Event log L , PN with places P , decay functions $f_p(\tau)$ for each place $p \in P$

Ensure: Set of timed state samples S

- 1: Initialize counting vector $C(\tau)$ to zero
 - 2: **for** each trace $g \in L$ **do**
 - 3: Reset $F(\tau)$, $C(\tau)$, and marking $M(\tau)$ to initial states
 - 4: **for** each event e_i in trace g **do**
 - 5: Calculate decay function responses $F(\tau) = \{f_p(\tau) \mid p \in P\}$
 - 6: Update $C(\tau)$ for token movements
 - 7: Update PN marking $M(\tau)$ based on transition fired by e_i
 - 8: Construct timed state sample $S(\tau) = F(\tau) \oplus C(\tau) \oplus M(\tau)$
 - 9: Add $S(\tau)$ to set of timed state samples S
 - 10: **end for**
 - 11: **end for**
 - 12: Return set of timed state samples S
-

As a result, the slope will not be overly flat or steep. In Algorithm3 $F(\tau)$ is a vector of decay functions for all places. $C(\tau)$ shows the number of tokens that have entered each place from time 0 to τ . When a token enters place p and time τ the corresponding value in $C(\tau)$ vector is updated. Here $M(\tau)$ is a vector representing the marking of a PN. So for each trace g and events in traces, the value of the aforementioned vectors are updated, and then the timed state sample $S(\tau)$ is constructed by concatenating the vectors. Consequently, a timed state sample, $S(\tau)$ provides a time-dependent description of a PN process state. It includes data regarding time-based token movements, such as token counts per location (loop information), the current PN state using the marking, and the last time a token entered a place in relation to the current time. In the last step of the algorithm, the $S(\tau)$ is input to the different NN with different architecture for predicting the next event.

3.5 Prediction

DREAM was used to predict the critical health outcomes for both pre-processed and non-processed event logs L . DREAM replays the event logs L on a process model and produces time information related to the variables which are called TSS. The TSS, demographic information, and severity scores were fed into the dense NN for prediction. The NN architecture differs by disease but remains the same for both pre-processed and unprocessed event logs L .

3.5.1 CAD disease

TSS are fed into a unique branch of one hidden layer with 200 neurons as shown in Figure2. The Dropout (DO) rate after the first layer was regularized at $DO = 0.2$. Demographic information was fed into a single hidden layer with 20 neurons and the same dropout rate. These were concatenated into a second layer with 90 neurons and the same dropout rate. The critical outcome which is predicted in this case is the mortality of ICU patients with CAD.

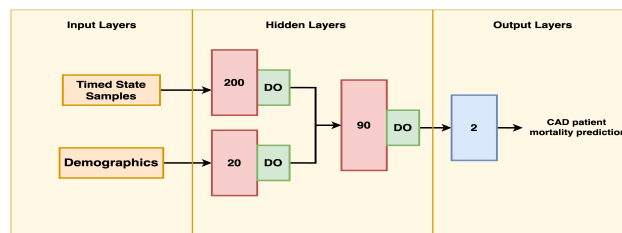


Figure 2: Architecture of the NN to predict CAD related outcome

3.5.2 HF disease

TSS, demographics information, and severity scores were fed separately to three branches each with three hidden layers (Figure3). A batch normalization layer was added after the first hidden layer for each branch with a dropout rate of 0.2. The output layer included a softmax activation function to predict unplanned 30-day readmission of ICU HF patients. The critical outcome predicted in this case was unplanned 30-day readmission of ICU patients with HF.

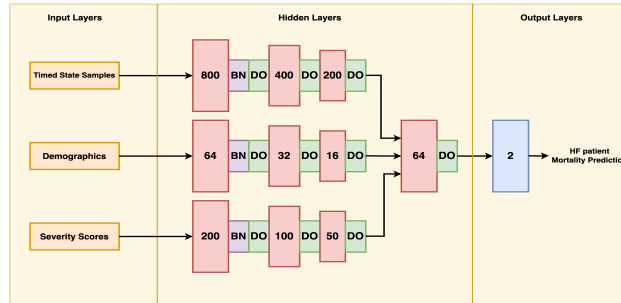


Figure 3: Architecture of the NN to predict HF related outcome

3.5.3 Diabetes

Each input layer is fed to an individual hidden layer branch before a hidden layer concatenates the branches and feeds it to two further layers. All hidden layers use a Rectified Linear Unit activation function (ReLU). The branched first hidden layers also have a batch normalization layer. Dropout layers with a rate of 0.4 for regularization are used. The output layer consists of a softmax activation function to output the patient’s probability of in-hospital mortality for diabetes patients. This architecture is shown in Figure4.

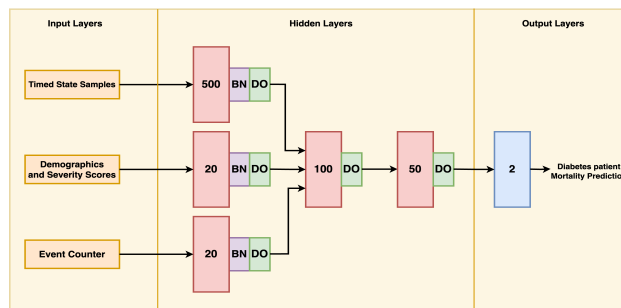


Figure 4: Architecture of the NN to predict Diabetes related outcome

3.5.4 COVID-19

TSS, demographics information and comorbidities were fed separately to two branches where the first branch contained three hidden layers with 90, 50 and 20 neurons respectively (Figure5). The first and second hidden layers each had a dropout layer with a rate of 0.2. The second branch also contained one hidden layer with 5 neurons. The two branches were concatenated to a branch with three hidden layers, containing 90, 50, and 20 neurons respectively. The dropout layer after the second concatenated hidden layer had a rate of 0.3. The output layer used a softmax activation function to predict mortality of COVID-19 patients every 6-hour during the first 72 hours after hospital admission.

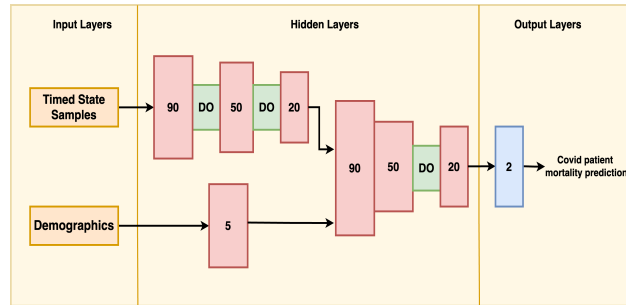


Figure 5: Architecture of the NN to predict COVID-19 related outcome

3.5.5 PI

In Figure 6, TSS were fed into two hidden layers. The first had 76 neurons and a subsequent dropout rate of $DO = 0.5$. The second hidden layer contained 20 neurons. The demographic information was fed into a single hidden layer of 5 neurons. Both layers were concatenated into two further layers with 96 and 10 neurons respectively. Between these two layers was a layer with a dropout rate of $DO = 0.5$. The outcome predicted in this case was the mortality of ICU patients diagnosed with PI 24 hours after being admitted to the ICU.

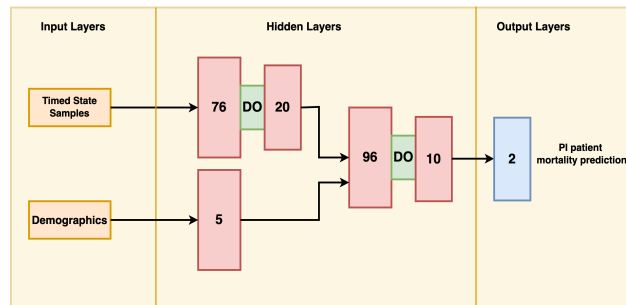


Figure 6: Architecture of the NN to predict PI related outcome

4 Evaluation

This section discusses experimental evaluation of the model to predict the critical health outcomes. Subsection one describes the datasets. Subsection two describes the modeling set up. Subsection three highlights the results.

4.1 Datasets

Data was obtained from MIMIC III (Medical Information Mart for Intensive Care) [27], a large database containing information relating to patients admitted to Beth Israel Deaconess Medical Center (BIDMC). This data includes vital signs, medications, laboratory measurements, observations and notes charted by care providers, fluid balance, procedure codes, diagnostic codes, imaging reports, hospital length of stay, survival data, and more [27]. Data was also obtained from UIH, a tertiary, teaching hospital in Chicago. This study was approved by The University of Illinois at Chicago (UIC) Institutional Review Board [18]. A summary of the datasets for each disease category is shown in Table 3.

Table 3: Summary of datasets by disease category

Disease	Total Numbers of Patients	Train	Test	Validation
HF	3,411	2,422	555	434
COVID-19	508	303	104	101
PI	1,153	681	336	136
CAD	2,176	1,202	674	300
Diabetes	2,435	1,552	609	274

4.2 Setup

RapidProM was used to run experiments [24] extending RapidMiner with process mining analysis capabilities. A concatenation algorithm’s threshold value of p^* was used to select the combinations of concurrent events for further concatenation steps.

The optimal value of p^* was based on the highest F-Measure value. The hyper-parameter optimization was conducted on 16 datasets using steps of 0.1. Of these, 13, found an optimal value of $p^* = 0.7$.

SM takes two threshold values: η and ϵ . These values were optimized based on the highest F-Measure values using steps of 0.1. Thresholds selected were $\eta = 0.4$ and $\epsilon = 0.1$.

Train and validation sets are required to discover a process model and train the NN. The validation set is used to select the best model. A test set is then used to evaluate model performance. A summary of the set up for training the NN for each disease category is shown in Table4.

Table 4: Summary of setup for training NN

Disease	Activation Function	Epoch	Batch Size	Optimizer
HF	ReLU	100	12	Adam
COVID-19	ReLU	350	10	Adam
PI	ReLU	350	50	RMSprop
CAD	ReLU	300	56	RMSprop
Diabetes	ReLU	200	256	Adam

We measured the quality of the process models with and without pre-processing using common metrics of fitness, precision, and F-Measure as proxies for accuracy, size, CFC, and structuredness, which indicate complexity.

The metric used to evaluate the model prediction is the AUC score which is equal to the probability that a classifier ranks a randomly chosen positive instance higher than a randomly chosen negative one. AUC is a better classification estimate than other common classification performance metrics [28]. Higher AUC scores indicate that a model is better at distinguishing between discharged patients and those who die. Furthermore, the 95% confidence interval (CI) for the AUC score is calculated using DeLong’s method [29].

4.3 Results

In our first experiments without pre-processing, we used the optimal threshold values found for the SM algorithm, plus raw event logs to discover process models. The model was fed to the DREAM algorithm to produce a TSS. The TSS, severity score and demographics were then fed to a NN for prediction.

For our second experiments, with pre-processing we applied the concatenation algorithm to raw event logs L using optimal thresholds values for the algorithm to produce modified event logs L . The modified event logs L were then fed to the SM algorithm with the aforementioned optimal threshold values to discover a process model, which was then fed to the DREAM algorithm to produce the TSS. The TSS, severity score and demographics were then fed to a NN for prediction.

Results of the evaluation are summarized in Table5. The F-Measure is calculated for different types of disease before and after the concatenation algorithm. In Table6, AUC and CI are calculated and in Table7 complexity is measured by

evaluating the size of the models, structuredness and CFC. We ran the Wilcoxon Test to determine whether improvements observed for evaluation metrics applied after concatenation were statistically significant or not ($p = 0.05$). Of 6 pre-processed datasets, 9 showed statistically significant differences in AUC scores. All 16 showed statistically significant differences in F-Measures and complexity metrics.

Table 5: Results in terms of F-Measure on event logs, and the Wilcoxon test results on improved cases to statistically identify significance level

Type of Disease	Evaluation Metrics		
	F-Measure		
	before concat	after concat	p-value
HF	0.821	0.830	0.048
PI	0.842	0.861	0.039
COVID 6hr	0.844	0.871	0.037
COVID 12hr	0.844	0.871	0.037
COVID 18hr	0.844	0.871	0.037
COVID 24hr	0.844	0.871	0.037
COVID 30hr	0.844	0.871	0.037
COVID 36hr	0.844	0.871	0.037
COVID 42hr	0.844	0.871	0.037
COVID 48hr	0.844	0.871	0.037
COVID 54hr	0.844	0.871	0.037
COVID 60hr	0.844	0.871	0.037
COVID 66hr	0.844	0.871	0.037
COVID 72hr	0.844	0.871	0.037
Diabetes	0.791	0.792	0.055
CAD	0.832	0.854	0.045

4.4 Discussion

To reduce concurrences and self-loops of the complex healthcare data, we applied a concatenation algorithm as a pre-processing step to improve data quality to improve the trustworthiness of prediction models for clinicians. We observed significant statistical improvements in AUC values, F-Measure and complexity metrics.

This was especially evident for the CAD and COVID-19 datasets which were more complex compared to other datasets. In those cases the predicted results improved by significant statistical amount of 2% for the AUC metric from our experiments.

One of the main advantages of a process mining approach is that it discovers a detailed process model which allows clinicians to comprehensively visualize the entire process patients (careflow) go through in a medical system. This is precisely why process mining has been preferred over other traditional machine learning methods. Process mining also accurately models temporal time-related information related to variables and utilizes them effectively as an input to the neural networks when other traditional techniques cannot. Lastly, process mining leverages the extensive and detailed medical history of patients from prior hospital admissions.

A limitation of the proposed approach is that it requires patients' medical history that small clinics and hospitals might not have. It also excludes patients with no prior hospital admissions like new patients and patients who are not admitted before the current hospital visit. Moreover, hospitals tend not to share patient data across outside hospital networks. Thus, the proposed approach best matches large hospital networks. In addition, the training, validation, and test sets all came from the MIMIC-III and UIH datasets. Therefore, using an independent dataset from a different health center or hospital would better test the performance of the model for future research.

Table 6: Results of the proposed model in terms of AUC and CI on event logs, and the Wilcoxon test results on the improved cases to statistically identify the level of significance

Type of Disease	Evaluation Metrics				
	AUC			CI	
	before concat	after concat	p-value	before concat	after concat
HF	0.930	0.947	0.045	[0.898- 0.960]	[0.910- 0.971]
PI	0.810	0.823	0.047	[0.768- 0.840]	[0.788- 0.850]
COVID 6hr	0.776	0.779	0.055	[0.678- 0.876]	[0.701- 0.790]
COVID 12hr	0.782	0.79	0.043	[0.685- 0.880]	[0.708- 0.850]
COVID 18hr	0.806	0.802	NA	[0.719- 0.901]	[0.788- 0.850]
COVID 24hr	0.799	0.791	NA	[0.698- 0.890]	[0.718- 0.870]
COVID 30hr	0.814	0.841	0.034	[0.718- 0.910]	[0.786- 0.855]
COVID 36hr	0.814	0.799	NA	[0.718- 0.900]	[0.778- 0.890]
COVID 42hr	0.817	0.817	NA	[0.701- 0.870]	[0.789- 0.860]
COVID 48hr	0.806	0.82	0.042	[0.738- 0.890]	[0.784- 0.880]
COVID 54hr	0.853	0.869	0.039	[0.758- 0.910]	[0.788- 0.890]
COVID 60hr	0.843	0.842	NA	[0.768- 0.870]	[0.748- 0.890]
COVID 66hr	0.875	0.881	0.046	[0.778- 0.940]	[0.798- 0.950]
COVID 72hr	0.900	0.915	0.045	[0.868- 1.00]	[0.870- 0.990]
Diabetes	0.873	0.861	NA	[0.851- 0.940]	[0.788- 0.890]
CAD	0.871	0.890	0.044	[0.831- 0.913]	[0.870- 0.923]

Table 7: Results of in terms of complexity metrics on event logs, and the Wilcoxon test results on the improved cases to statistically identify the level of significance

Type of Disease	Evaluation Metrics								
	Size			Struct.			CFC		
	before concat	after concat	p-value	before concat	after concat	p-value	after concat	before concat	p-value
HF	70	46	0.032	142	121	0.034	71	66	0.032
PI	151	89	0.037	301	190	0.036	88	67	0.035
COVID 6hr	1001	401	0.031	2325	998	0.033	142	71	0.031
COVID 12hr	1001	401	0.031	2325	998	0.033	142	71	0.031
COVID 18hr	1001	401	0.031	2325	998	0.033	142	71	0.031
COVID 24hr	1001	401	0.031	2325	998	0.033	142	71	0.031
COVID 30hr	1001	401	0.031	2325	998	0.033	142	71	0.031
COVID 36hr	1001	401	0.031	2325	998	0.033	142	71	0.031
COVID 42hr	1001	401	0.031	2325	998	0.033	142	71	0.031
COVID 48hr	1001	401	0.031	2325	998	0.033	142	71	0.031
COVID 54hr	1001	401	0.031	2325	998	0.033	142	71	0.031
COVID 60hr	1001	401	0.031	2325	998	0.033	142	71	0.031
COVID 66hr	1001	401	0.031	2325	998	0.033	142	71	0.031
COVID 72hr	1001	401	0.031	2325	998	0.033	142	71	0.031
Diabetes	68	35	0.034	121	101	0.043	70	69	0.035
CAD	98	79	0.032	132	97	0.031	73	66	0.038

5 Conclusion

Healthcare data is complex and have many concurrences and loops. This makes predicting healthcare outcomes difficult, because data quality is poor. By using concatenation algorithm as a pre-processing step, data complexity decreased, improving the performance of process discovery algorithms by recommending a probability-based concatenation of events, with concurrent relations. Thus, it can predict critical healthcare outcomes more accurately.

Predicting critical health outcomes allows medical stakeholders to provide optimal treatment for patients to increase life expectancy. For instance, if a patient is predicted to die or readmit, investing many resources on them will not be optimal. Moreover, in cases when we can predict a patient's outcome sooner, medical stakeholders can expedite treatment to save a patient's life. Furthermore, knowing outcomes with high AUC would allow medical teams improve treatment decisions and allocate medical resources more effectively.

We used 16 healthcare datasets and fed them to the SM algorithm to discover the process model. Moreover, the pre-processing step was also applied to the same event logs, and the resultant event logs were used by the SM algorithm to discover a process model. We then measured the F-Measure and complexity of the models for both cases. We fed both pre-processed and raw data to the DREAM algorithm for prediction, and compared the results. In cases where improvements were observed in evaluation metrics, the Wilcoxon Test was run to measure the level of significance. Results indicated that the pre-processing step increased F-Measure values and decreased the complexity of the models statistically. Prediction of critical health outcomes improved as well. These results demonstrate that using a pre-processing step improves data quality, hence improves the process model and prediction modeling results. Using an effective process mining / deep learning algorithm like the DREAM algorithm also, ensures medical history and time information related to variables are not ignored which can predict outcomes more accurately.

In future work, we plan to use other pre-processing approaches to see their effects on data quality and predicting critical health outcomes. We plan to find techniques that optimally adjust parameter values automatically, rather than using hyper-parameter optimization currently in favor. We would also validate the proposed approach using healthcare datasets. Finally, MIMIC-III and UIH datasets contains useful information like clinical notes and images that can be converted into event logs and fed to models as inputs.

Appendix: Notations

a	Event
A	Finite set of all events
α	Decay rate
α_p	Decay rate for a specific place p
β	Constant parameter of a decay function
$C(\tau)$	Token counting vector from time 0 to τ each element represents the number of tokens that entered a specific place
d	Attribute
d_{ts}	Timestamp attribute
D	Finite set of all possible attributes
$\Delta_{max}(L)$	Maximum observed trace duration in an event log L
Δ_p	Difference of τ and τ_p
$\delta_p(g)$	function of average time between a token is consumed in place p until a new token is produced in p based on an input trace g
E	Event instance vector
e	An instance of E
η	SM threshold which controls concurrency relations
ϵ	SM threshold which controls filtering process
$f_p(\tau)$	Decay function of place p
$F(\tau)$	Decay function response vector
g	Case or trace
G	Finite set of all possible traces
L	Event log which is a set of traces
$L_{i,j}$	j^{th} event instance in the i^{th} trace of an event log L
ℓ	label of each event
λ	function that retrieves the label of each event

$\lambda_p(g)$	Number of tokens a place p produces when replaying a trace g
$M(\tau)$	Vector representing the marking of a PN
$mean()$	Arithmetic mean function
N	Set of all possible event instances
$\nu_d(E)$	Function returning value of attribute d of event instance E
p	Place
P	Set of all places
PN	Mathematical definition of a labeled PN
$p\star$	Threshold value for concatenation algorithm
$S(\tau)$	Timed state sample at time τ
S	Set of timed state samples
τ	Time
τ_p	Most recent time that a token entered place p
$v_p(g)$	number of tokens a place p produces when replaying a trace g
$e_i \oplus e_j$	Concatenated event for e_i and e_j
$p(e_i \rightarrow e_j)$	The probability that e_j happens instantly after e_i
$p(e_i e_j)$	probability of the frequency that event e_j which occurs immediately after event e_i

Acknowledgment

The authors would like to thank all contributors of MIMIC-III for providing the public EHR dataset.

References

- [1] Pishgar, M., Theis, J., Del Rios, M. et al. Prediction of unplanned 30-day readmission for ICU patients with heart failure. *BMC Med Inform Decis Mak* 22, 117 (2022). <https://doi.org/10.1186/s12911-022-01857-y>
- [2] Ghasemi M, Amyot D. Process mining in healthcare: a systematised literature review. *Int J Electron Healthc.* 2016;9:60.
- [3] M. Pishgar, M. Razo, J. Theis and H. Darabi, "Process Mining Model to Predict Mortality in Paralytic Ileus Patients," 2021 International Conference on Cyber-Physical Social Intelligence (ICCSI), 2021, pp. 1-6, doi: 10.1109/ICCSI53130.2021.9736217.
- [4] J. Theis, W. Galanter, A. Boyd and H. Darabi, "Improving the In-Hospital Mortality Prediction of Diabetes ICU Patients Using a Process Mining/Deep Learning Architecture," in *IEEE Journal of Biomedical and Health Informatics*.
- [5] Pishgar, M., Harford, S., Theis, J. et al. A process mining- deep learning approach to predict survival in a cohort of hospitalized COVID-19 patients. *BMC Med Inform Decis Mak* 22, 194 (2022). <https://doi.org/10.1186/s12911-022-01934-2>
- [6] M. Sani, S. van Zelst, and A. Van Der, "Improving the performance of process discovery algorithms by instance selection," *Comput. Sci. Inf. Syst.*, vol. 17, no. 3, pp. 927–958, 2020.
- [7] M. Pishgar, M. Razo and H. Darabi, "Improving Process Discovery Algorithms Using Event Concatenation," in *IEEE Access*, vol. 10, pp. 69072-69090, 2022, doi: 10.1109/ACCESS.2022.3185235.
- [8] S. Baharlouei, S. Patel, and M. Razaviyayn, "f-FERM: A scalable framework for robust fair empirical risk minimization," in *Proc. Int. Conf. Learn. Representations (ICLR)*, 2024.
- [9] N. Ashrafi, Y. Liu, X. Xu, Y. Wang, Z. Zhao, and M. Pishgar, "Deep learning model utilization for mortality prediction in mechanically ventilated ICU patients," medRxiv, Mar. 2024. [Online]. Available: <https://doi.org/10.1101/2024.03.20.24304653>.
- [10] JC. Brown, TE. Gerhardt, E. Kwon . Risk Factors For Coronary Artery Disease. 2021 Jun 5. In: StatPearls [Internet]. Treasure Island (FL): StatPearls Publishing; 2022 Jan-. PMID: 321192

- [11] N. Ashrafi, A. Abdollahi, G. Placencia, and M. Pishgar, "Process mining/deep learning model to predict mortality in coronary artery disease patients," medRxiv, Jun. 2024. [Online]. Available: <https://www.medrxiv.org/content/10.1101/2024.06.26.24309553v1>.
- [12] Mozaffarian DBE, Go A, Arnett D, Blaha M, Cushman M, et al. Heart disease and stroke statistics-2016 update: a report from the American Heart Association. *Circulation*. 2016;133:e38–360.
- [13] J. Zhang, H. Li, N. Ashrafi, Z. Yu, G. Placencia, and M. Pishgar, "Prediction of in-hospital mortality for ICU patients with heart failure," medRxiv, Jun. 2024. [Online]. Available: <https://doi.org/10.1101/2024.06.25.24309448>.
- [14] S. Mohan, C. Thirumalai and G. Srivastava, "Effective Heart Disease Prediction Using Hybrid Machine Learning Techniques," in *IEEE Access*, vol. 7, pp. 81542-81554, 2019, doi: 10.1109/ACCESS.2019.2923707.
- [15] Desautels T, Das R, Calvert J, Trivedi M, Summers C, Wales DJ, et al. Prediction of early unplanned intensive care unit readmission in a UK tertiary care hospital: a cross-sectional machine learning approach. *BMJ Open*. 2017;7(9): e017199.
- [16] L. Wei, X. Yongtao, H. Jianhu, L. Lina, T. Yiqing, Y. Weihui, C. Yi, and C. Wei, "Causes and prognosis of chronic intestinal pseudo-obstruction in 48 subjects: a 10-year retrospective case series," *Medicine* 97, 2018.
- [17] Taubenberger JK, Morens DM. 1918 Influenza: the mother of all pandemics. *Rev Biomed*. 2006;17(1):69–79.
- [18] Galanter, W., Rodríguez-Fernández, J.M., Chow, K. et al. Predicting clinical outcomes among hospitalized COVID-19 patients using both local and published models. *BMC Med Inform Decis Mak* 21, 224 (2021). <https://doi.org/10.1186/s12911-021-01576-w>.
- [19] M. Chen, Y. Hao, K. Hwang, L. Wang, and L. Wang, "Disease prediction by machine learning over big data from healthcare communities," *IEEE Access*, vol. 5, pp. 8869–8879, 2017.
- [20] W. van der Aalst, "Data science in action," in *Process Mining: Data Science in Action*, W. van der Aalst, Ed., Berlin, Germany: Springer, 2016, pp. 3–23.
- [21] J. Theis, and H. Darabi, "Decay Replay Mining to Predict Next Process Events," *IEEE Access*, 7, 119787–119803, 2019.
- [22] J. Mendling, *Metrics for Process Models: Empirical Foundations of Verification, Error Prediction, and Guidelines for Correctness*. Cham, Switzerland: Springer, 2008.
- [23] J. Cardoso, "Business process control-flow complexity: Metric, evaluation, and validation," *Int. J. Web Services Res.*, vol. 5, no. 2, pp. 49–76, Apr. 2008.
- [24] W.M.vanderAalst,A.Bolt,andS.J.vanZelst,"RapidProM:Mineyour processes and not just your data," 2018, arXiv:1703.03740.
- [25] J. Mendling, H. A. Reijers, and W. M. P. van der Aalst, "Seven process modeling guidelines (7PMG)," *Inf. Softw. Technol.*, vol. 52, pp. 127–136, Feb. 2010, doi: 10.1016/j.infsof.2009.08.004.
- [26] R.Confort.BPMNMiner: Automated Discovery of BPMN Process Models with Hierarchical Structure. Accessed: Aug. 1, 2022. [Online]. Available: <https://github.com/raffaeleconforti/ResearchCode>
- [27] Johnson AE, Pollard TJ, Shen L, Lehman LWH, Feng M, Ghassemi M, Mark RG. MIMIC-III, a freely accessible critical care database. *Sci Data*. 2016;3(1):1–9.
- [28] N. Srivastava, G. Hinton, A. Krizhevsky, I. Sutskever, and R. Salakhutdinov, "Dropout: A simple way to prevent neural networks from overfitting," *J. Mach. Learn. Res.*, vol. 15, no. 1, pp. 1929–1958, Jan. 2014.
- [29] S. M. Lundberg, and L.Su-In. "A unified approach to interpreting model predictions." *Advances in Neural Information Processing Systems*, 2017.